Defect Transfer from Nanoparticles to Nanowires

Sven Barth,[1,2,3] John J. Boland[2,4] and Justin D. Holmes[1,2]*

[1]Materials and Supercritical Fluids Group, Department of Chemistry and the Tyndall National Institute, University College Cork, Cork, Ireland.

[2]Centre for Research on Adaptive Nanostructures and Nanodevices (CRANN), Trinity College Dublin, Dublin 2, Ireland.

[3]Institute for Materials Chemistry, Vienna University of Technology, 1060 Vienna, Austria.

[4]School of Chemistry, Trinity College Dublin, Dublin 2, Ireland

*Corresponding author: j.holmes@ucc.ie, tel: +353 214 903608, fax: +353 214 274097

ABSTRACT

Metal-seeded growth of 1D semiconductor nanostructures is still a very active field of research, despite the huge progress which has been made in understanding this fundamental phenomenon. Liquid growth promoters allow control of the aspect ratio, diameter and structure of 1D crystals via external parameters, such as precursor feedstock, temperature and operating pressure. However the transfer of crystallographic information from a catalytic nanoparticle seed to a growing nanowire has not been described in the literature. Here we define the theoretical requirements for transferring defects from nanoparticle seeds to growing semiconductor nanowires, and describe why Ag nanoparticles are ideal candidates for this purpose. We detail in this paper the influence of solid Ag growth seeds on the crystal quality of Ge nanowires, synthesized using a supercritical fluid growth process. Significantly, under certain reaction conditions {111} stacking faults in the Ag seeds can be directly transferred to a high percentage of <112> oriented Ge nanowires, in the form of radial twins in the semiconductor crystals. *Defect transfer* from nanoparticles to nanowires could open up the possibility of engineering 1D nanostructures with new and tuneable physical properties and morphologies.

KEYWORDS: Germanium, Nanowire, Solid-Phase-Seeding, SFSS, Silver, Nanocrystal, Defects.

One-dimensional (1D) semiconductor nano-architectures with tunable morphologies, dimensions, crystallographic phases and orientation are of tremendous interest for a broad range of current and future applications [1], including energy harvesting [2] and generation [3], sensing [4], optics [5] and electronics [6]. The design and controlled growth of 1D nanostructures will enable the distinct physical and chemical properties of these building blocks to be utilized. Several metal supported/catalyzed-growth mechanisms, such as vapor-solid-solid (VSS) [7], vapor-liquid-solid (VLS) [8], supercritical-fluid-liquid-solid (SFLS) [9] and supercritical-fluid-solid-solid (SFSS) [10], have been used to describe and interpret the growth of 1D nanostructures by vapor, liquid and supercritical fluid phase techniques. Recently, the growth of longitudinally heterostructured nanowires was demonstrated to be controllable with sharp interfaces between segments [11], intentional twinning [12, 13] and kinking [14].

Theoretically a solid seed should enable the transfer of crystal information to a growing material similar to the defect-supported growth of nanowires "seeded" by screw dislocation translations from epitaxial substrates to the growing material [15]. There are therefore distinct features of the solid phase seeding mechanism that potentially offer opportunities for the controlled processing of nanomaterials with new physical properties. Usually VSS nanowire growth processes require lower synthesis temperatures compared to VLS growth, using the same seed material, leading to minimal contamination of the semiconductor; as both the diffusivity and equilibrium solubility of metals in semiconductors increases with temperature [16]. The high dopant concentrations in semiconductor nanowires can result from unintentional incorporation of atoms from the metal seed material, as described for the Al-catalyzed VLS growth of Si nanowires which can in turn be depressed by solid-phase seeding [17]. In addition, the creation of very sharp interfaces between group IV semiconductor segments has been achieved by solid seeds [18], whereas the traditionally used liquid Au particles often leads to compositional tailing of the interface [19]. Korgel *et al.* also described the superior size retention of metal seeds in a SFSS nanowire growth process, when compared to a SFLS process using Au colloids [20]. To date, there have been no reports in the literature describing defect generation or transfer from a

metal particle seed to a growing semiconductor nanowire.

The transfer of a defect from a particle to a growing nanowire will occur only if the seeding nanoparticle meets certain requirements, such as (i) the structure and lattice constant should be predictable and match with the growing nanowire, without undergoing major changes during reaction with the growth material (in our case, germanide formation); (ii) a moderate solubility of the growing material in the seed should be ensured; (iii) the energy for twin formation in the nanoparticle seeds should be moderate and (iv) the growth temperature is low enough to prevent melting and subsequent VLS-type growth. Figure 1(a) maps these requirements onto a range of potential seed materials. Some of the transition metals form one or more germanides, which does not meet requirement (i) above and does not allow controlled interface formation between the wire and seed. Seed elements that are known to undergo variations in composition and phase induced by germanide formation, and for which there is a very limited tendency to form twin structures, are highlighted in green in figure 1(a), and are not potential materials for defect transfer. A second group of metals have a low melting point (blue/grey color code) which is less than the temperature required for Ge nanowire formation by the thermal decomposition of diphenylgermane in supercritical media and are excluded on this basis. Zinc is immiscible with germanium below the eutectic temperature and therefore it was not suitable for our studies. This leaves 3 potential metals (Ag, Al and Au) which have sufficient solid solubility for Ge incorporation and diffusion (a "pocket" on the metal rich side of the phase diagram). The candidates are highlighted by a golden color in figure 1(a). The lattice constants are similar and all of the Ge-metal combinations are reported to have an epitaxial relationship with the growing germanium. However, twinning energies are low for only the noble metals Ag and Au [21]. Therefore Al was not considered further in our experiments. Comparing the Ag and Au seed choices with our experimental setup, which requires higher temperatures, we could rule out Au because it forms a low melting liquid eutectic where the solid-liquid transition can be as low as 280°C. Figure 1(b) shows a flow chart detailing the aforementioned requirements leading to the selection of Ag as a seeding material. Germanide formation

usually includes the structural rearrangement of atoms in the seed prior to nanowire growth, which will change the particle properties. Additionally, binary seeds are less predictable in terms of extended defect generation due to generally limited literature data on most of these compounds. Our literature survey revealed that Ag should be an ideal candidate to demonstrate the ability of defect transfer as outlined below.

We describe in this paper, the SFSS formation of 1D Ge nanostructures using Ag particles as growth promoters and the transfer of defects from the nanoparticle seeds to growing crystalline nanowires. Surprisingly, there is only one recent report published to date on the growth of 1D Ge crystals using Ag as a growth promoter in a gas phase approach [22], as the phase diagram resembles the well known Si-Ag and Si-Al systems [23; 24]. The binary Ag-Ge system shows no eutectic at low temperatures (< 640 ºC), however there is a pocket at the Ag-rich side. The composition of the solid solution of Ge in the fcc-Ag matrix is temperature dependent and allows the incorporation of up to 9 at% below the eutectic point. A small expansion of the lattice by incorporation of 3.5-4.5 % Ge at the given nanowire growth temperature range between 370-430 ºC is anticipated [24]. As mentioned above, Ag is especially receptive to forming stacking faults [25], leading to observed twinning in the nanocrystals synthesized in this study. To increase the defect density in the seed material we synthesized Ag nanocrystals with a mean diameter of ~6.3 nm, which displayed very few defects, due to the small domain size (figure 2(a)), however minor defects cannot be ruled out as described in the literature for fcc metal nanoparticles [26, 27]. These small, low defect Ag nanoparticles were subsequently annealed at the nanowire growth temperature (~400 °C) to cause them to fuse into larger seeds (mean diameter ~25-30 nm as shown in figure S2) with a high number of stacking faults [28]. Very small Ag particles of between 2-4 nm in diameter were not considered in this study as starting colloids because nanoparticles of these dimensions would be expected to fuse together very quickly in a liquid-like behavior process [29]. Therefore, in order to stay in an all-solid regime, the seed size was not further decreased. TEM evidence (figure 2(a) inset) shows that the Ag seeds are coagulated and twinning can be observed after simple heat treatment

under similar supercritical conditions used for nanowire growth. Ag nanocrystals, with a nominal diameter of 6.3 (±0.5) nm were synthesized by the thermal decomposition of silver oleate in a high boiling point solvent [30]. The Ag particles were deposited onto a silicon substrate and dried at 180 ºC under vacuum leading to desorption of the surfactant molecules, responsible for good adhesion to the substrate and destabilization, leading to easier interparticle fusion. The *in-situ* fusion approach was chosen to create a high number of stacking faults [31] and to reduce the effect of a decreasing defect density by annealing [32]. The native oxide layer on the silicon substrate was not removed prior to the deposition of silver nanoparticles, which would have had an effect of pre-alignment of the Ag nanoparticles with respect to the silicon lattice [32]. As expected from the phase diagram, effective growth of Ge nanowires via the thermolysis of diphenylgermane in supercritical toluene was achieved, as shown in a typical SEM image (figure 2(b)). The TEM image in the inset of figure 2(b) shows no noticeable tapering of the nanowires and the formation of high aspect ratio nanostructures. The growth temperature was well below the eutectic temperature of 640 ºC and size-dependent melting point depression should not lead to liquefied alloys at these temperatures (difference of >200 ºC). In this study Ge nanowires with radial dimensions between 15-30 nm (> 80 %) were observed. Interestingly, a major growth direction of these nanowires was along the <112> axis (~40 %), which is known to show lamellar {111} twinning along the axis and represents indeed the identical planes expected to be present in Ag crystals. <111>-oriented nanowires (~40 %) and <110> growth axis were also observed (figure S1). The observed nanowire growth directions are significant as generally <112>-oriented Ge nanowires only make up a minor part of a sample for Au or Ni-supported growth (< 5 %) [20, 33].

The most significant fingerprint for an effective defect transfer is the high number of axially twinned Ge nanowires in our samples, which is shown by several TEM images in figure S3. We observed this twinning for all of the <112> nanowires studied; between 40-45 % of nanowires in a sample. HRTEM analysis at the growth front of the nanowires with the Ag seed was undertaken to evaluate the influence of the nanoparticles on the high number of axially twinned Ge nanowires. {111} stacking faults are

responsible for the layered structure along the length of the nanowires, which is also occasionally visible for <112> Au-seeded (VLS or SFLS) group IV semiconductor nanowires grown via CVD and supercritical fluid processes (figure S4) [34, 35]. However, for a molten eutectic mixture, such as the Au-Ge system where no seed-mediated twinning effect is possible, these wires are scarce (< 5 %) and reports on Ge nanowires exhibiting this lamellar twinning are very limited. Similar structural defects are described in a couple of papers dealing with Si nanowires [36, 37]. Davidson *et al.* associated the occurrence of this lamellar twinning to nucleation events at the liquid-solid interface of the molten Au-Ge eutectic and the substrate [38] and step formation after solidification at the interface was observed [39]. Even though the step formation resembles the findings we describe in the following section, there was no twinning observed and reported in the Au particles after solidification. The growth of Si nanowires from twinned Au particles has been shown by *in-situ* experiments, however the low eutectic temperature of Au-Si led to the melting of these particles and loss of any structural information to suggest defect transfer [40]. The transfer of information from a twinned nanowire to the small volume of a Ag particle could be the another explanation for the data we describe. However, given the slightly lower energy barrier for generating stacking faults in Au compared to Ag, and the similar dimensions of Au and Ag used to growth nanowires, comparable yields of defective nanowires would be expected with both seed types if the mechanism of formation was due to defective nanowires forcing the metal particle to form the {111} stacking faults upon cooling of the system. The absence of this transfer effect in our Au-seeded Ge nanowires represents indirect proof that the small catalyst volume of the Ag seeds are indeed forcing the nanowire material to respond, suggesting a nanoparticle to nanowire transfer process.

The structural relationship between the two elements is described in detail for Al-Ge alloys [41] and to a lesser extent Ag-Ge systems [42]. These early reports dealt with quenched alloys of these elements and show phase separation below the melting point, where Ge crystals, with partially rod-like appearance, align along specific axis in the Ag or Al matrix without the creation of defects in the 3 D metal host material. Data relating to twinning energies in the alloys formed in many metal-

semiconductor systems used for solid phase seeding, such as the $NiGe_2$ phase, are not available, but for all elemental metals suitable for Ge nanowire growth the calculated energy values are the lowest for Ag [21] as already mentioned above.

Energy dispersive X-ray (EDX) analysis of the nanocrystals terminating the nanowires showed Ge concentrations below 1 % and (111) lattice spacings of 0.234 nm, which is in good agreement with the reference value of pure Ag crystals (0.236 nm, PDF 03-0921). The Ag nanoparticles terminating the ends of the Ge nanowires often exhibited non-hemispherical regular forms, which supports nanowire growth via the SFSS mechanism. Figure 3 shows a triangular Ag crystal at the tip of a single crystalline nanowire. The corresponding Fast Fourrier transformation (FFT) patterns were used to determine the orientation of the crystals. For <111>-oriented wires there is a coincidence grain boundary between the Ge and the Ag crystals in the same orientation. The misfit and strain between the 5 Ge and 7 Ag {111} planes illustrated in the image is accommodated by dislocations at the interface. Similar findings after the solidification of Au seeds are described in the literature [43]. The resulting lattice misfit of ~1.3 % between 5 Ge and 7 Ag {111} planes is probably marginally lower during growth due to the expansion of the Ag fcc-lattice by Ge impurities forming a solid solution. The visible Moiré pattern at the interface is caused by the superposition of the Ge crystal attached to the Ag single crystal in this region. Even though the longitudinal twinning of <110> nanowires is generally not prominent and not observed in our investigations, these events cannot be ruled out. For instance, {111} stacking faults have been described as being present along the axis of <110> Ge nanorods formed in a confined 3 D metal matrix [33, 41].

The regular appearance of twin planes in the Ag seed particles and the corresponding Ge nanowires grown from them is shown in figure 4(a). Slight diffraction contrasts are visible in the Ag particles and the body of the Ge nanowires shown. The low resolution image already illustrates the interaction of the defects in the Ag particles and the twins in the grown Ge nanowires by their location in the crystals (similar axis and common interface). The interfaces of the segments in the Ge crystal can be identified

as (111) stacking faults by the corresponding FFT pattern of individual segments and the twinned region as shown in figure 4(b). Figure 4(c) shows a high resolution image of the Ag-Ge region in a lamellar twinned Ge nanowire. The nanoparticle exhibits twinning planes, which can be identified as {111} planes via site selective FFT patterns as shown in the insets in figure 4(b), similar to twinning and stacking faults observed in Ge nanowires which grow along the <112> axis. Comparing the FFT pattern of the Ge crystallites and the Ag seeds in the FFT reveals an offset of ~2.9 degrees. Considering the strain between both cubic crystals, due to a lattice mismatch of ~3.5 % (4 Ag and 3 Ge {111} planes), the binary system can relax for thin wires by tilting of the Ag nanoparticle off-axis, possibly during the cooling of the system and depletion of Ge in the Ag seed matrix, along with the {111} planes in the nanocrystal. The resulting quasi-widening of the interface lattice spacing helps to minimize strain between both crystals. This effect is not mandatory, as seen in wires with a larger diameter leading to almost no tilting of the particle material (figure S5a). Figure S5(d) shows the twinning in a seed particle and a nanowire at the growth front, as well as the same feature at a distance of ~600 nm from the growth front, illustrating the same twinning pattern along the length of the wires. In addition, figures 4(d) and S4 (a-d) represent further examples of defect transfer from Ag seeds to Ge nanowires. Figure 4(d) clearly shows an identical brightness contrast pattern in the Ag seed and Ge nanowire. The effect is caused by the diffraction from the different crystallite segments due to their orientation to the impinging electron beam. The contrast reversal from wire to the particle is due to the slightly different diffraction of the electron beam by the two crystal lattices (slightly detached nanoparticle). In most of these twinned terminating metal particles the interface is not smooth and twins can also result in steps, as shown in the inset in figure 4(a) to form stable crystal terminating surfaces. The creation of a defect site in the semiconductor can be observed at these kink sites at the interface. The steps are a side effect of the defects in the seed crystal, due to an energetically favored arrangement of atoms at the metal particle grain boundary [44], and a reason for defect formation in the Ge lattice. However, the (112) surface is intrinsically unstable in group IV semiconductors [45]. Metal deposition at higher temperatures in an

UHV environment can also lead to faceting of (112) single crystal surfaces but this effect is not the underlying cause of defect formation in the growing Ge nanowires described herein. In addition, the size of the facets described in the literature is temperature dependent and smallest for low temperatures in the range of the growth temperature employed [46]. In turn, a Ag particle without defects should wet the surface as well, but no data are available in the literature describing how large Ag particles respond after cooling to room temperature. Unfortunately, literature data dealing with the formation of faceting and metal-semiconductor interactions of these unstable surfaces are scarce. The high number of <112>-oriented Ge nanowires observed in our study suggests a preferential nucleation of these unusual wires when compared to other growth seeds which could be an effect of the twinning. This impact on the growing lattice at the most favored slip plane in the semiconductor leads to a progression of this imperfection beyond the interface. In addition, the defect sites in the seed particle could either exhibit a preferential diffusion path for Ge atoms to be incorporated at the interface as described for enhanced kinetics in chemical diffusion along the interfaces in bicrystals [47] and along the {111} surfaces in fcc Cu, when compared to other crystal directions [22]. Another explanation for the effective defect transfer, given the rough/slanted interface, would include a layer by layer growth of (111) layers underneath the metal particle, where the edges provide nucleation sites for the simultaneous growth of Ge layers on each subsection of the twinned semiconductor to metal particle interface [48]. The particle to nanowire interface is generally very dynamic, constantly fluctuating, forming and annihilating facets as seen in dynamic TEM studies for the solid-phase seeding of Si nanowires via palladium-silicide particles [49]. The wetting of non-planar or stepped surfaces always favors the attachment of diffusing species on step edges or surface defects. Given an uneven Ge-Ag interface, the arrangement continuously provides nucleation sites at the interface, which might be comparable to a screw-dislocation driven growth, of 1D nanostructures [50].

In summary, we have demonstrated that defects can be induced in growing semiconductor nanowires by solid phase seeding processes. Ag nanoparticle-supported Ge nanowire growth showed a high

percentage of 1D crystals with {111} twinning defects along their axis, which is reflected in the defects in the Ag nanoparticles terminating the nanowires at the growth front. To our knowledge, this is the first report of *defect-transfer* from a metal nanoparticle into a growing Ge nanowire. Our study on solid phase seeding should provide the basis which will enable controlled defect generation in semiconductor nanowires along their axis. The segmented nanowires potentially exhibit new and controllable physical properties, such as altered mechanical strength and electrical characteristics. Furthermore, controlled incorporation of these axial stacking faults could open up the possibility of selective doping of the nanowire interfaces due to enhanced impurity incorporation at these interfaces as demonstrated for Au atoms located in <112> oriented nanowires [51]. In addition, the increased popularity of solid phase seeding to control heterostructure formation could also be affected by a control of defects in the nanoparticles and the scenarios described herein. Given the immense variety of potential binary alloy seeds we can assume that the described effect is not limited to a specific seed-nanowire material combination. For further improvement of this strategy, a defined number of twin planes should be achieved by the defined control of twinning events in the particle [52], which is however beyond the scope of the presented paper. These investigations have to be seen as a proof-of-concept and not a sophisticated approach to control defects one by one on a large or even industrial scale. Even though most researchers are focused on the growth and integration of single crystalline "perfect" nanowires in devices of industrial interest, we strongly believe that a potential control over defects will provide some novel opportunities to alter the materials properties.

ACKNOWLEDGMENT

We acknowledge financial support from the Science Foundation Ireland (Grants 07/RFP/MASF710 and 08/CE/I1432). This research was also enabled by the Higher Education Authority Program for Research in Third Level Institutions (2007-2011) via the INSPIRE programme. Dr Markus Boese and the Advanced Microscopy Laboratory (AML) in CRANN are thanked for their assistance in electron microscopy investigations.

Supporting Information available:

Detailed experimental procedure, characterization techniques and equipment used. TEM images of the synthesized Ge nanowires with longitudinal defects and statistical data of the determined growth direction are presented.

REFERENCES

[1] Barth, S.; Hernandez-Ramirez, F.; Holmes, J. D.; Romano-Rodriguez, A. *Progress in Materials Science* **2010**, *55*, 563.
[2] Kempa, T. J.; Tian, B. Z.; Kim, D. R.; Hu, J. S.; Zheng, X. L.; Lieber, C. M. *Nano Lett.* **2008**, *8*, 3456.
[3] Wang, Z. L.; Song, J. H. *Science* **2006**, *312*, 242.
[4] Prades, J. D.; Jimenez-Diaz, R.; Hernandez-Ramirez, F.; Barth, S.; Cirera, A.; Romano-Rodriguez, A.; Mathur, S.; Morante, J. R. *Appl. Phys. Lett.* **2008**, *93*,
[5] Huang, M. H.; Mao, S.; Feick, H.; Yan, H. Q.; Wu, Y. Y.; Kind, H.; Weber, E.; Russo, R.; Yang, P. D. *Science* **2001**, *292*, 1897.
[6] Cui, Y.; Zhong, Z. H.; Wang, D. L.; Wang, W. U.; Lieber, C. M. *Nano Lett.* **2003**, *3*, 149.
[7] Persson, A. I.; Larsson, M. W.; Stenstrom, S.; Ohlsson, B. J.; Samuelson, L.; Wallenberg, L. R. *Nat. Mater.* **2004**, *3*, 677.
[8] Wagner, R. S.; Ellis, W. C. *Appl. Phys. Lett.* **1964**, *4*, 89.
[9] Holmes, J. D.; Johnston, K. P.; Doty, R. C.; Korgel, B. A. *Science* **2000**, *287*, 1471.
[10] Tuan, H. Y.; Lee, D. C.; Hanrath, T.; Korgel, B. A. *Nano Lett.* **2005**, *5*, 681.
[11] Bjork, M. T.; Ohlsson, B. J.; Sass, T.; Persson, A. I.; Thelander, C.; Magnusson, M. H.; Deppert, K.; Wallenberg, L. R.; Samuelson, L. *Nano Lett.* **2002**, *2*, 87.
[12] Hao, Y.; Meng, G.; Wang, Z. L.; Ye, C.; Zhang, L. *Nano Lett.* **2006**, *6*, 1650.
[13] Caroff, P.; Dick, K. A.; Johansson, J.; Messing, M. E.; Deppert, K.; Samuelson, L. *Nat. Nanotechnol.* **2009**, *4*, 50.
[14] Tian, B. Z.; Xie, P.; Kempa, T. J.; Bell, D. C.; Lieber, C. M. *Nat. Nanotechnol.* **2009**, *4*, 824.
[15] Morin, S. A.; Jin, S. *Nano Lett.* **2010**, *10*, 3459.
[16] Graff, K. (2000). Metal Impurities in Silicon-Device Fabrication, 2nd ed., Springer.
[17] Ke, Y.; Weng, X. J.; Redwing, J. M.; Eichfeld, C. M.; Swisher, T. R.; Mohney, S. E.; Habib, Y. M. *Nano Lett.* **2009**, *9*, 4494.
[18] Wen, C. Y.; Reuter, M. C.; Bruley, J.; Tersoff, J.; Kodambaka, S.; Stach, E. A.; Ross, F. M. *Science* **2009**, *326*, 1247.
[19] Clark, T. E.; Nimmatoori, P.; Lew, K. K.; Pan, L.; Redwing, J. M.; Dickey, E. C. *Nano Lett.* **2008**, *8*, 1246.
[20] Tuan, H. Y.; Lee, D. C.; Hanrath, T.; Korgel, B. A. *Chemistry of Materials* **2005**, *17*, 5705.
[21] Rosengaard, N. M.; Skriver, H. L. *Phys. Rev. B* **1993**, *47*, 12865.
[22] Hong, C. Y.; Tsai, S. F.; Chang, H. C.; Lin, W. T.; Wu, K. H. *J. Nanosci. Nanotechnol.* **2010**, *10*, 4773.
[23] Wittemann, J. V.; Munchgesang, W.; Senz, S.; Schmidt, V. *J. Appl. Phys.* **2010**, *107*, 096105.
[24] Elliott, R.; Shunk, F. *Journal of Phase Equilibria* **1980**, *1*, 47.
[25] Major, S. S.; Grosskre.Jc. *Jpn. J. Appl. Phys.* **1968**, *7*, 574.
[26] Elechiguerra, J. L.; Reyes-Gasga, J.; Yacaman, M. J. *J. Mater. Chem.* **2006**, *16*, 3906.
[27] Hofmeister, H.; Dubiel, M.; Tan, G. L.; Schicke, K. D. *physica status solidi (a)* **2005**, *202*, 2321.
[28] Okitsu, K.; Ashokkumar, M.; Grieser, F. *The Journal of Physical Chemistry B* **2005**, *109*, 20673.
[29] Zuo, J. M.; Li, B. Q. *Physical Review Letters* **2002**, *88*, 255502.
[30] Moh, K. (2009). Synthesis and characterization of metallic and oxidic nanostructures. Saarbruecken, Saarland University; Germany.
[31] Radziuk, D.; Grigoriev, D.; Zhang, W.; Su, D. S.; Mohwald, H.; Shchukin, D. *J. Phys. Chem. C* **2010**, *114*, 1835.
[32] Li, B. Q.; Zuo, J. M. *Phys. Rev. B* **2005**, *72*, 085434.
[33] Hanrath, T.; Korgel, B. A. *Small* **2005**, *1*, 717.
[34] Hanrath, T.; Korgel, B. A. *Adv. Mater.* **2003**, *15*, 437.
[35] Lopez, F. J.; Hemesath, E. R.; Lauhon, L. J. *Nano Lett.* **2009**, *9*, 2774.

[36] Conesa-Boj, S. N.; Zardo, I.; Estradé, S. N.; Wei, L.; Jean Alet, P.; Roca I Cabarrocas, P.; Morante, J. R.; Peiró, F.; Morral, A. F. I.; Arbiol, J. *Crystal Growth & Design* **2010**, *10*, 1534.
[37] Cayron, C.; Den Hertog, M.; Latu-Romain, L.; Mouchet, C.; Secouard, C.; Rouviere, J.-L.; Rouviere, E.; Simonato, J.-P. *Journal of Applied Crystallography* **2009**, *42*, 242.
[38] Davidson, F. M.; Lee, D. C.; Fanfair, D. D.; Korgel, B. A. *J. Phys. Chem. C* **2007**, *111*, 2929.
[39] Liu, X. H.; Wang, D. W. *Nano Res.* **2009**, *2*, 575.
[40] Kim, B. J.; Tersoff, J.; Wen, C. Y.; Reuter, M. C.; Stach, E. A.; Ross, F. M. *Physical Review Letters* **2009**, *103*, 155701.
[41] Douin, J.; Dahmen, U.; Westmacott, K. H. *Philos. Mag. B-Phys. Condens. Matter Stat. Mech. Electron. Opt. Magn. Prop.* **1991**, *63*, 867.
[42] Dahmen, U.; Hetherington, C. J. D.; Radmilovic, V.; Johnson, E.; Xiao, S. Q.; Luo, C. P. *Microscopy and Microanalysis* **2002**, *8*, 247.
[43] Mathur, S.; Barth, S.; Werner, U.; Hernandez-Ramirez, F.; Romano-Rodriguez, A. *Advanced Materials* **2008**, *20*, 1550.
[44] Chen, K.-C.; Wu, W.-W.; Liao, C.-N.; Chen, L.-J.; Tu, K. N. *Science* **2008**, *321*, 1066.
[45] Baski, A. A.; Whitman, L. J. *J. Vac. Sci. Technol. A* **1995**, *13*, 1469.
[46] Nabbefeld, T.; Wiethoff, C.; Heringdorf, F.-J. M. Z.; Hoegen, M. H.-V. *Appl. Phys. Lett.* **2010**, *97*, 041905.
[47] Germain, V.; Li, J.; Ingert, D.; Wang, Z. L.; Pileni, M. P. *The Journal of Physical Chemistry B* **2003**, *107*, 8717.
[48] Battey, J. F.; Baum, R. M. *Physical Review* **1955**, *100*, 1634.
[49] Hofmann, S.; Sharma, R.; Wirth, C. T.; Cervantes-Sodi, F.; Ducati, C.; Kasama, T.; Dunin-Borkowski, R. E.; Drucker, J.; Bennett, P.; Robertson, J. *Nat Mater* **2008**, *7*, 372.
[50] Sears, G. W. *Acta Metallurgica* **1955**, *3*, 361.
[51] Allen, J. E.; Hemesath, E. R.; Perea, D. E.; Lensch-Falk, J. L.; Li, Z. Y.; Yin, F.; Gass, M. H.; Wang, P.; Bleloch, A. L.; Palmer, R. E.; Lauhon, L. J. *Nat. Nanotechnol.* **2008**, *3*, 168.
[52] Wiley, B. J.; Xiong, Y. J.; Li, Z. Y.; Yin, Y. D.; Xia, Y. A. *Nano Lett.* **2006**, *6*, 765.

Figures

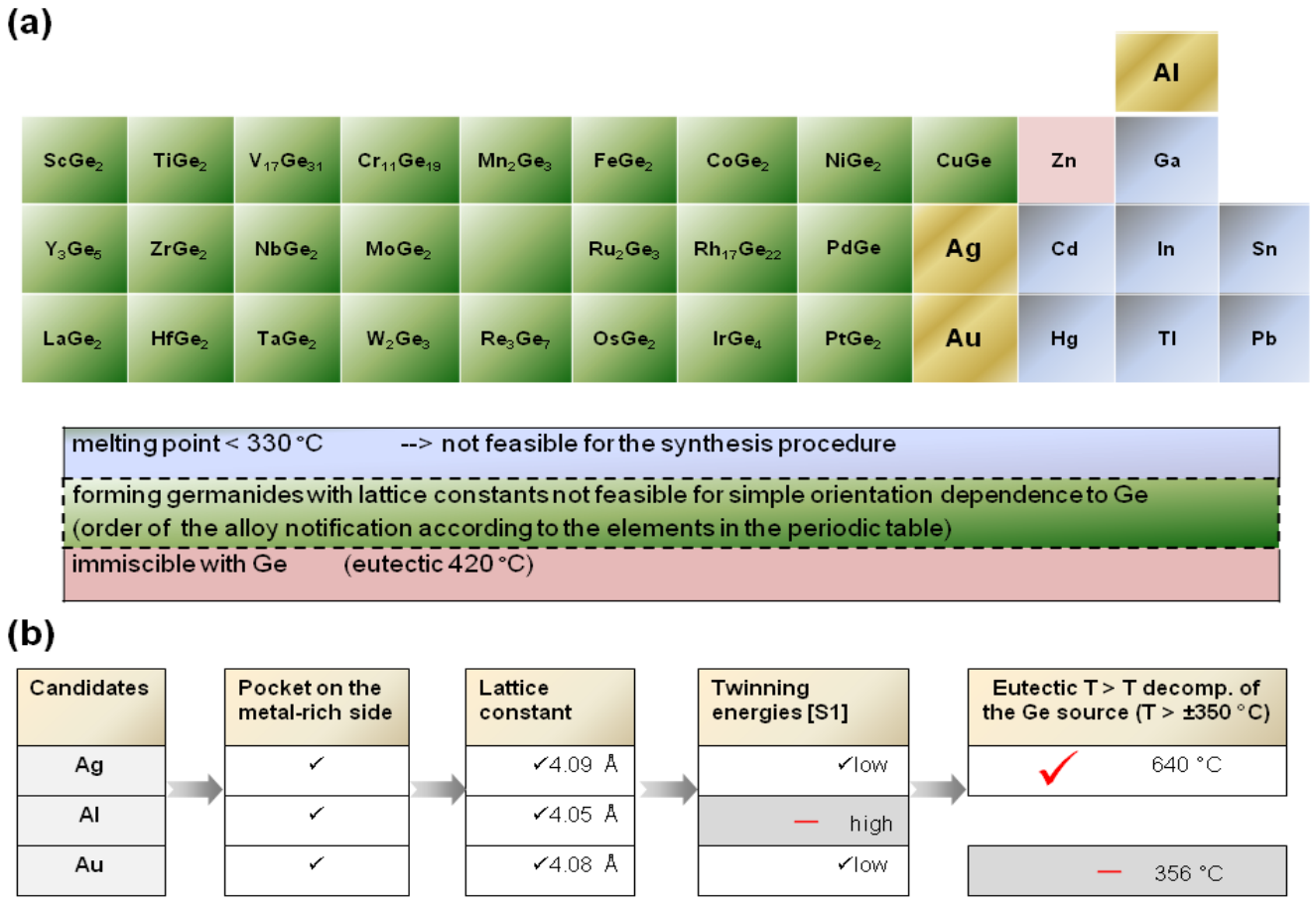

Figure 1. *Selecting an Appropriate Metal Seed:* (a) Overview of solid metal germanium alloys (Ge rich phase) and other physical properties of potential metal seeds present at the synthetic window for Ge NW growth using diphenylgermane precursor in supercritical toluene (350-500 °C). (b) shows a flow chart leading to the choice of Ag seeds to demonstrate the theory of defect transfer from the seed to the growing nanowire

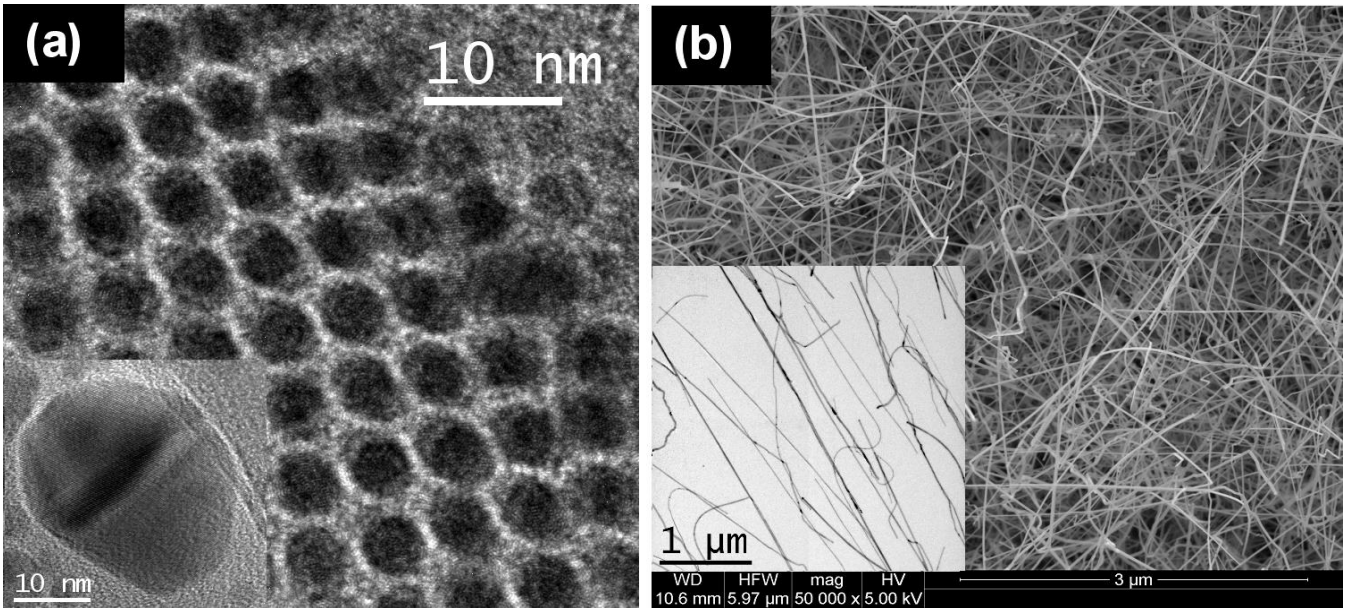

Figure 2. (a) Silver nanocrystals (mean diameter 6.3 ± 0.5 nm) used as growth seeds for germanium nanowire synthesis. The lower resolution TEM image shows particles in underfocus to show a not perfect size selective synthesis. The majority of the particles are nearly monodisperse. The inset illustrates a 30 nm Ag crystal after heat treatment at 400 °C showing a twin structure. (b) SEM image illustrating the effective seeding of Ge nanowires by Ag nanoparticles and the TEM inset shows the constant nanowire diameter without tapering.

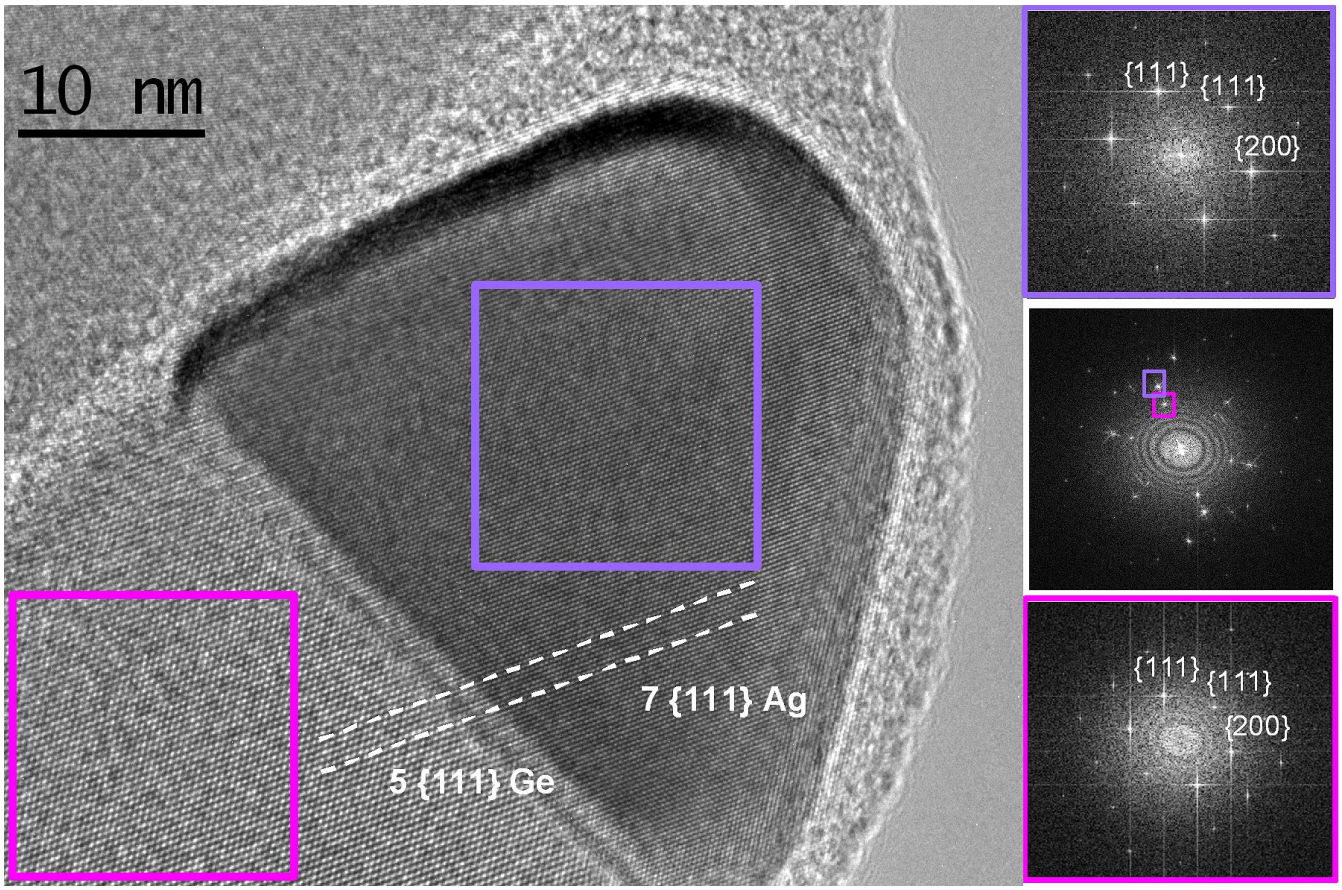

Figure 3. The HRTEM image shows the highly crystalline nature of both the nanowire and the metal nanoparticle. A Moiré pattern can be seen at the interface between both crystals due to a slight overlapping region. The interface FFT pattern displays the excellent crystallinity of the nanowire with a <111> growth direction and the alignment of Ag and Ge crystals.

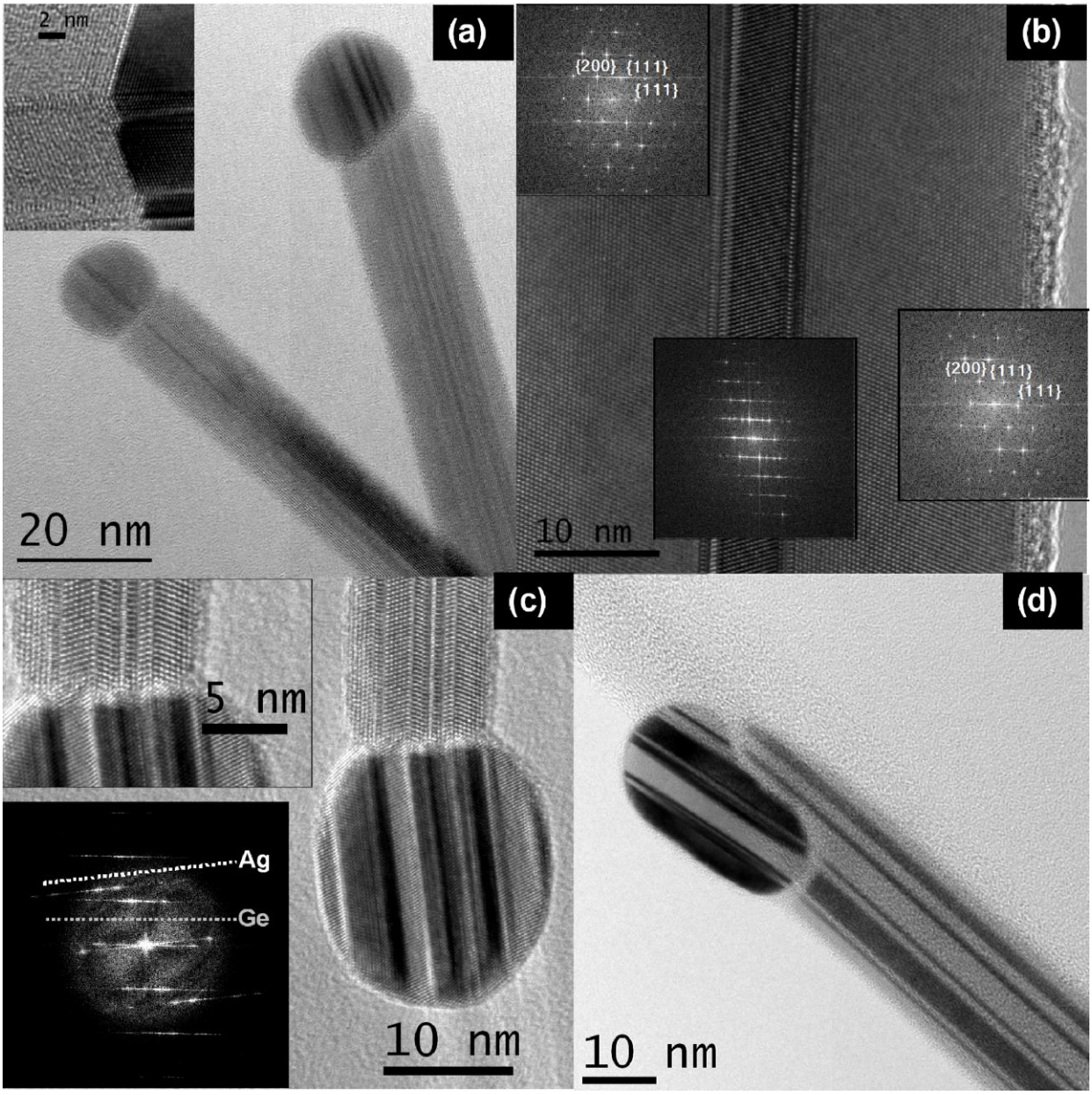

Figure 4. *Defect Transfer in Ag-Seeded Ge Nanowires:* (a) TEM image showing two nanowire-seed regions with brightness contrast at locations of the stacking faults along their axes in both silver seeds and germanium nanowires due to twinning. The inset shows the interface between the seed particle with steps, which influences the Ge lattice of the growing nanowire, (b) shows a TEM image of a Ge nanowires with FFT of the different segments and a combined FFT illustrating the {111}twin planes. The HRTEM in (c) demonstrates the defect transfer from the Ag seeds to the Ge nanowires, the different segments are clearly visible with similar thickness. The lower resolution TEM in (d) is

acquired a few tenth of a degree off-axis and therefore the different crystal orientations appear in bright and dark contrast. The particle is detached from the nanowire body, but the corresponding segments are distinguishable and show the identical brightness contrast pattern in the Ag seed and Ge nanowire.